



# Vibration and Stability Analysis of Functionally Gradient Flow Pipe with Axial Motion

Jie Zhou<sup>1,2</sup>(✉), Haowen Mou<sup>1</sup>, Junchao Gao<sup>1</sup>, and Xueping Chang<sup>2</sup>

<sup>1</sup> Tianjin Aerospace Relia Technology Co., Ltd., Tianjin 300000, China  
17713653269@163.com

<sup>2</sup> College of Mechanical and Electrical Engineering, Southwest Petroleum University,  
Chengdu 610065, China

**Abstract.** The axially moving functionally graded pipe is widely used in many fields of industry, and its vibration and stability analysis is the key to its design. In this paper, the vibration characteristics and stability of functionally graded pipes with axial motion are analyzed. Based on the extended Hamilton variational principle, the dynamic equation of the pipe with internal flow velocity, material volume fraction index and axial velocity is established. The modified Galerkin method is used to solve the dynamic equation. The influence of the internal flow velocity, material volume fraction index, axial velocity and acceleration on the dynamic characteristics and stability of the system is analyzed. The characteristic curves of volume fraction index, axial velocity, acceleration and natural frequency are given. The results show that the natural frequency and critical velocity of the system increase with the increase of volume fraction index, and the designed volume fraction index can adjust the natural frequency of FGM pipeline system. When the system has axial acceleration, the greater the acceleration, the system will reach the critical value of axial instability in a short time.

**Keywords:** Functionally Graded Materials · Volume Fraction Index  $n$  · Axial Acceleration · Critical Velocity · Natural Frequency

## 1 Introduction

Functionally gradient materials (FGM) [1] are composed of two or more different materials. In functionally gradient materials, power series, S-shaped function and exponential function are mainly used to describe the changes of mechanical properties of functionally gradient materials in functionally gradient structures [2]. The mechanical properties and research of functionally gradient materials are reviewed in References [2]. Its volume fraction index changes smoothly and continuously along the preferred direction [3, 4]. In the study reported in References [5], the linear vibration of FGM pipe conveying fluid is studied.

The results show that the stability of the pipe is significantly improved when the conventional isotropic material is replaced by a functional gradient material (FGM). In fact, the improved stability of FGM pipes is mainly due to their increased stiffness. Deng et al. [6] analyzed the instability of multispan viscoelastic pipes made of

functional gradient materials using the wave propagation method and the reverberation ray matrix algorithm. Tang and Yang [7] investigated the dynamics and stability of a bi-directional FGM infused nanotube. The governing equations and corresponding boundary conditions were obtained using Hamilton's principle and solved by differential product method. The results showed that the bi-directional material distribution can significantly change the critical flow rate, fundamental frequency and stability. Wang and Liu [8] evaluated the effect of power-law exponents on the deflection and stability of a clamped FGM pipeline by using the Sin method. An and Su [9] analyzed the linear vibration and amplitude of a functionally graded pipeline for transporting fluids by using the generalized integral transform method.

The dynamic response of the axial motion system under the action of moving mass has important practical research value. Li Weiming et al. studied the dynamic response of the simply supported beam under the continuous velocity change of the moving mass. [10], Wang Yingze et al. studied the vibration of the barrel under the action of multiple moving masses. [11], Liu Ning et al. studied the vibration characteristics of the axially moving cantilever beam under the action of moving mass. [12], Wu et al. studied the dynamic response of the axially moving beam under the moving mass based on the finite element method. [13], CHEN et al. studied the vibration analysis of the axially moving beam and the chord [14]. DING et al. derived several different forms of the control equations of the axially moving beam, and analyzed the differences between the control systems by numerical analysis. [15], Qi Yafeng, Liu Ning et al. studied the vibration response analysis of the axially moving simply supported beam [16]. In the above research, the influence of the axial velocity on the vibration characteristics of the fluid-conveying pipe is rarely considered.

The article takes the axial motion functional gradient flow tube as the research object, and the description of the mechanical properties of its material is described by a power series, and the FGM linear Euler-Bernoulli model containing the inward flow velocity with axial motion is established. The governing equations of the system were derived using Hamilton's principle. Then the Galerkin method is utilized to solve its dynamical system. Finally, the effects of several parameters on the vibration characteristics and stability of the axial motion functional gradient flow tube are discussed.

## 2 Establishment of Mathematical Models

Considering the mathematical model of the axial velocity of the FMG pipe, an analysis model is established as shown in Fig. 1. A functionally graded axially moving pipe with an average radius of  $r$  and a length of  $l$ ,  $r_i$  and  $r_o$  represent the inner and outer diameters of the pipe,  $U$  represents the velocity of the fluid, and  $v$  represents the axial velocity of the pipe. The pipeline adopts the Euler-Bernoulli beam model. In this paper, the power series is used to describe the effective performance change of functionally graded materials along the thickness direction. When the mechanical properties change in the form of power function, the effective mechanical properties of the pipeline can be expressed as [17].

$$P_f = P_m V_m + P_c V_c \quad (1)$$

in which  $P_m, P_c$  is the material properties of metals and ceramics (such as Young's modulus and mass density),  $V_m$  and  $V_c$  are the volume fractions of metals and ceramics, respectively, and the composition is expressed as

$$V_c = \left( \frac{R_0 - r}{R_0 - R_i} \right)^n, \quad V_c + V_m = 1 \tag{2}$$

Among them,  $n$  is the volume fraction power-law index; the labels  $i$  and  $o$  represent the inner and outer layers, respectively. Since the mechanical properties of the functional gradient flow transfer pipe are in the radial direction along the pipe, the effective bending stiffness and mass per unit length of the functional gradient material can be written as [17, 18]

$$(EI)^* = \int E z^2 dA = \int_0^{2\pi} \int_{R_i}^{R_o} E(r) r^2 \sin^2 \theta r dr d\theta \tag{3}$$

$$m^* = \int \rho dA = \int_0^{2\pi} \int_{R_i}^{R_o} \rho(r) r dr d\theta \tag{4}$$

where:  $(EI)^*$  is the effective bending stiffness of the functionally graded tube;  $m^*$  is the mass per unit length of the functionally graded tube.

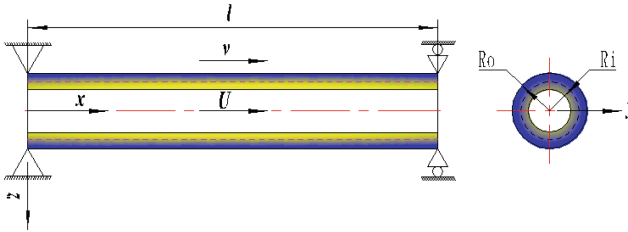


Fig. 1. Model of axial motion system

The dynamic modeling of the model is carried out by Hamilton principle.

$$\delta \int_{t_1}^{t_2} (T - V) dt + \int_{t_1}^{t_2} \delta W dt = 0 \tag{5}$$

In this study, the tube has an axial velocity, so the tube has an axial displacement. The change rate of the deflection  $w(x, t)$  with time, that is, the calculation of the lateral velocity and acceleration should be based on the field velocity. The change rate of the field coordinate  $x$  with time is to calculate the derivative of the deflection to time, and the change rate of the  $x$  coordinate must be considered. Therefore:

$$\frac{dw}{dt} = \frac{\partial w}{\partial t} + v \frac{\partial w}{\partial x} \tag{6}$$

$$\frac{d^2 w}{dt^2} = \frac{\partial^2 w}{\partial t^2} + 2 \frac{\partial^2 w}{\partial x \partial t} v + \frac{\partial w}{\partial x} \dot{v} + \frac{\partial^2 w}{\partial x^2} v^2 \tag{7}$$

The fluid kinetic energy can be expressed as:

$$T_f = \frac{1}{2} M_f \int \left[ \left( \frac{\partial w}{\partial t} + U \frac{\partial w}{\partial x} \right)^2 + U^2 \right] dx \quad (8)$$

The potential energy of the functionally graded tube without considering the effect of gravity can be expressed as:

$$V_p = \frac{1}{2} \int (EI)^* \left( \frac{\partial^2 w}{\partial x^2} \right)^2 dx \quad (9)$$

The kinetic energy of the functionally graded pipe can be expressed as:

$$T_p = \frac{1}{2} m^* \int \left( \frac{dw}{dt} \right)^2 dx \quad (10)$$

By substituting Eq. (6), (8), (9), (10) into Eq. (5), the dynamic governing equations of the system can be obtained:

$$(EI)^* \frac{\partial^4 w}{\partial x^4} + (M_f U^2 + m^* v^2) \frac{\partial^2 w}{\partial x^2} + m^* v \frac{\partial w}{\partial x} + 2(M_f U + m^* v) \frac{\partial^2 w}{\partial x \partial t} + (M_f + m^*) \frac{\partial^2 w}{\partial t^2} = 0 \quad (11)$$

### 3 Numerical Calculation

The vibration model of the axial power tube is a complex time-varying system, and the natural frequency and vibration shape of the structure are constantly changing with time, so the Galerkin method is used to approximate the solution, so the bending displacement of the beam can be expressed as Fig. 2:

$$w(\xi, \tau) = \sum_{i=1}^n \varphi_i(\xi) q_i(\tau) \quad (12)$$

Where  $q_i(\tau)$  ( $\tau=1, 2, 3 \dots n$ ) is the reduced generalized displacement, and  $\varphi_i(\xi)$  represents the modal function of the  $i$  th order of the system and satisfies the boundary condition. In this paper, we assume that:

$$\varphi_i(\xi) = \sin(n\pi x/l) \quad (13)$$

Substituting Eqs. (12) and (13) into Eq. (11), multiplying both sides by  $\varphi_j(\xi)$  at the same time, and then integrating on the interval  $[0, l]$ , we get:

$$\mathbf{M}\ddot{\mathbf{q}} + \mathbf{C}\dot{\mathbf{q}} + \mathbf{K}\mathbf{q} = 0 \quad (14)$$

where,  $\mathbf{q} = (q_1, q_2, q_3 \dots q_n)$ ,  $\mathbf{M}$ ,  $\mathbf{C}$ ,  $\mathbf{K}$  are mass matrix, damping matrix and stiffness matrix, respectively.

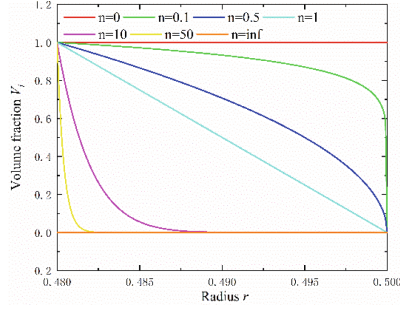


**Fig. 2.** Volume fraction  $V_i$  of inner material with different volume fraction index  $n$  change along the radial direction

Where:

$$\mathbf{M} = \begin{bmatrix} \mathbf{I} & \mathbf{0} \\ \mathbf{0} & \mathbf{I} \end{bmatrix} \quad \mathbf{C} = \begin{bmatrix} 2(M_f U + m^* v)B & 0 \\ 0 & 2(M_f U + m^* v)B \end{bmatrix} \quad (15)$$

$$\mathbf{K} = \begin{bmatrix} (EI)^* \Lambda + (M_f U^2 + m^* v^2)C^* + m^* v B & 0 \\ 0 & (EI)^* \Lambda + (M_f U^2 + m^* v^2)C^* + m^* v B \end{bmatrix} \quad (16)$$

$$\mathbf{C}_{ij}^* = \begin{cases} -(i\pi/l)^2 & i=j \\ 0 & i \neq j \end{cases} \quad \Lambda_{ij} = \begin{cases} (i\pi/l)^4 & i=j \\ 0 & i \neq j \end{cases} \quad \mathbf{B}_{ij} = \begin{cases} \frac{4ij}{i^2-j^2} & i+j \text{ is odd} \\ 0 & i+j \text{ is even} \end{cases} \quad (17)$$

where,  $C_{ij}^*$ ,  $\Lambda_{ij}$ ,  $B_{ij}$  are the matrix elements of row  $i$  and column  $j$ . The solution of Eq. (14) can be assumed as

$$\mathbf{q} = \mathbf{S} * \exp(i\omega t) \quad (18)$$

where,  $\mathbf{S}^* = (S_1, S_2, S_3, \dots, S_n)$ , Substituting Eq. (17) into Eq. (14), we can get:

$$\left( -\omega^2 \mathbf{M} + i\omega \mathbf{C} + \mathbf{K} \right) \mathbf{S}^* = 0 \quad (19)$$

Equation (19) has an asymmetric solution, so the determinant of the matrix coefficient must be 0.

$$\left| -\omega^2 \mathbf{M} + i\omega \mathbf{C} + \mathbf{K} \right| = 0 \quad (20)$$

## 4 Numerical Results Calculation and Discussion

### 4.1 Example Verification

The equation is dimensionless

$$\frac{\partial^4 \eta}{\partial \xi^4} + (u^2 + V^2) \frac{\partial^2 \eta}{\partial \xi^2} + \frac{\partial^2 \eta}{\partial \tau^2} + \gamma \frac{\partial \eta}{\partial \xi} + 2(u\sqrt{\beta} + V\sqrt{\delta}) \frac{\partial^2 \eta}{\partial \tau \partial \xi} = 0 \quad (21)$$

where:

$$u = \sqrt{\frac{M}{(EI)^*}} UL \quad V = \sqrt{\frac{m^*}{(EI)^*}} \nu L \quad \beta = \frac{M}{M + m^*} \quad \delta = \frac{m^*}{M + m^*} \quad \gamma = \dot{\nu} \frac{m^*}{(EI)^*} L^3 \tag{22}$$

When  $\sigma = 0, V = 0, \delta = 0, \gamma = 0$ , the model is a pipe conveying model without considering gravity and internal and external damping. In this state, the natural frequency and critical flow velocity of different flow velocity  $U$  are calculated (Tables 1 and 2).

**Table 1.** Comparison of dimensionless natural frequencies [19]

$U$	$\omega$	numerical results	Literature Results
$U = 0$	$\omega_1$	9.8696	$\pi^2$
	$\omega_2$	39.4784	$4\pi^2$

**Table 2.** Comparison of dimensionless critical velocity [19]

$U_{cr}$	Present results	Literature Results
The first modal frequency	3.14	$\pi$
The second-order modal frequency	6.28	$2\pi$

**Table 3.** Study material parameters

Material	$\rho_P (Kg/m^3)$	E(GPa)	G(GPa)
SiC	3210	440	188
Ti-6Al-4V	4515	115	44.57

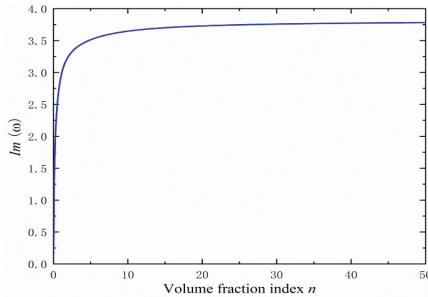
It can be seen from the results of the above table that when  $U = 0$ , the dimensionless natural frequencies of the first two orders are 9.8698 and 39.4784, which are consistent with the results of Reference [19]. Therefore, the program has certain accuracy in solving the complex frequency of the system. When  $\beta = 0.1$ , the dimensionless critical flow velocities corresponding to the first-order modal frequency and the second-order modal frequency are 3.14 and 6.28, which are consistent with the results of Reference [19], and the correctness of the algorithm is verified.

### 4.2 Example Analysis

Here, Deng [11] wave propagation method and reverberation ray matrix algorithm are selected to solve the computational parameters of the multi-span viscous multifunctional

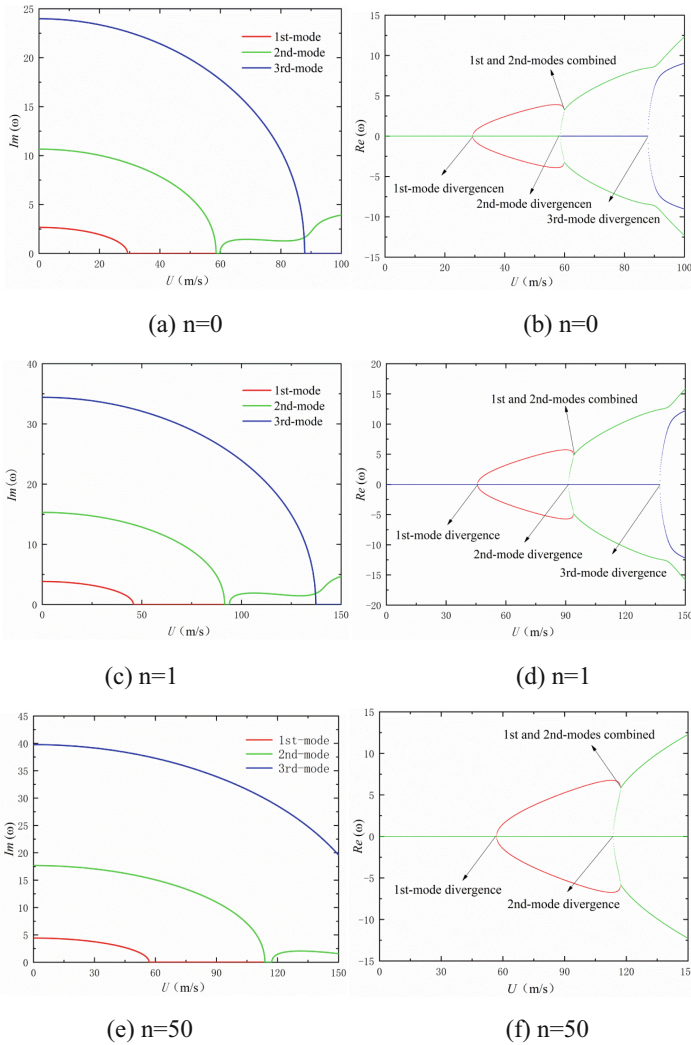
gradient flow tube, and the materials of the functional gradient are selected to be composed of SiC and Ti-6Al-4V. Since the material of the functional gradient changes into a gradient in the direction of the thickness, so in the functional gradient tube, the volume fraction of the SiC decreases from the outer surface gradually until it is reduced to zero. The volume fraction of the Ti-6Al-4V gradually decreases from the inner surface until it is reduced to zero.

Figure 3 depicts the variation of the natural frequency with the volume fraction index  $n$ . The system frequency increases with the increase of the volume fraction index, and the frequency is strongly affected by the volume fraction index when the volume fraction index  $n$  is between 0 and 10, and it is gradually reduced by the volume fraction index after  $n$  is greater than 10, and the frequency is almost unaffected by the volume fraction index when  $n = 50$ . From Table 3, it can be known that the Young's modulus of SiC is much larger than that of Ti-6Al-4V, and it can also be seen from Fig. 1 that when the volume fraction index is less than 10, the content of SiC changes faster with the increase of the index  $n$ , which has a larger effect on the dynamic properties of the system. When the volume fraction index  $n$  is greater than 10,  $V_i$  is gradually reduced by the influence of the index  $n$ . When the index  $n$  tends to infinity,  $V_i$  is almost unaffected by the index  $n$ . Therefore, we can conclude that the natural frequency of the functional gradient conveying pipeline is more sensitive to the volume fraction index  $n$  in the stage of lower flow velocity. As the volume fraction index  $n$  increases, its effect on the intrinsic frequency and stability of the pipe decreases. After the index  $n > 50$ , it has almost no effect on the dynamics of the functional gradient pipeline.



**Fig. 3.** Variation of natural frequency with functional gradient fractional index  $n$

Figure 4 shows the change of the first three natural frequencies of the functionally graded material tube with the flow rate under the action of different volume fraction index  $n$ . In the form obtained in this paper, the imaginary part  $Im(\omega)$  of the frequency is the vibration frequency of the pipeline, and the real part  $Re(\omega)$  of the frequency represents the growth or attenuation of the vibration response. The stability of the system can be determined by the real and imaginary parts of the natural frequency. When  $Im(\omega) > 0$ ,  $Re(\omega) = 0$ , the system is in a stable state; When  $Im(\omega) = 0$ ,  $Re(\omega) < 0$ , the system is in static instability. When  $Im(\omega) < 0$ ,  $Re(\omega) < 0$ , the system is in dynamic instability. It can be seen from the fig.(a) that when  $n = 0$ , the first-order modal instability occurs at  $U = 29.3 \text{ m/s}$ . When the flow rate continues to increase to  $U = 58.6 \text{ m/s}$ , the first-order

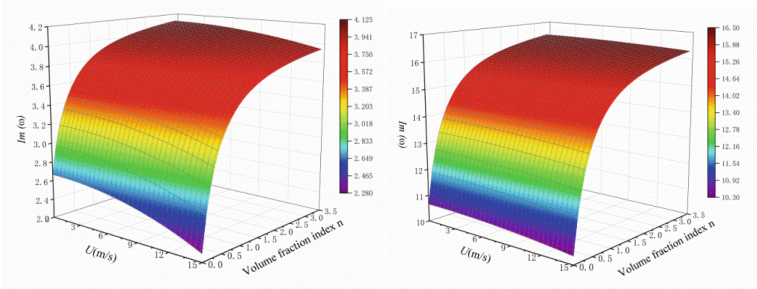


**Fig. 4.** Relationship between natural frequency and flow velocity under different volume fraction index

modal frequency and the second-order modal frequency overlap. The imaginary part of the frequency is positive and the real part of the frequency is negative, indicating that the system has a coupled dynamic instability. It can be seen from Fig. 4 (c) that when  $n = 1$ , the first-order modal instability occurs at  $U = 59.8 \text{ m/s}$ . It can be seen from Fig. 4 (e) that when  $n = 10$ , the first-order modal instability velocity  $U = 55.5 \text{ m/s}$ . It can be seen from Fig. 4 (g) that when  $n = 50$ , the first-order modal instability velocity occurs at  $U = 56.9 \text{ m/s}$ . In different volume fraction index  $n$ , when  $U < 59.8 \text{ m/s}$ , the system does not occur dynamic instability. The above analysis shows that the volume fraction index  $n$  of the functionally graded material has a great influence on the natural frequency and critical

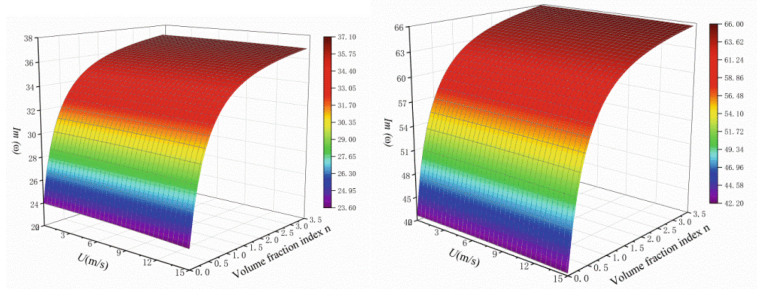


flow velocity of the system. The natural frequency and critical flow velocity of the system increase with the increase of the volume fraction index  $n$ . In practical engineering, the natural frequency of the system can be changed by adjusting the volume fraction index  $n$ , which has important guiding significance for the application of FGM in practical engineering.



(a) The 1st-order modal frequency

(b) The 2nd-order modal frequency



(c) The 3rd-order modal frequency

(d) The 4th-order modal frequency

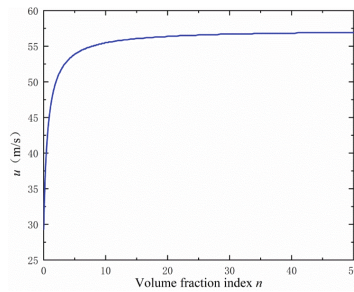
**Fig. 5.** Variation of the first four modal frequencies of the system with velocity and  $n$

Figure 5 is the first four natural frequencies of the system with the change of the fluid flow rate and the volume fraction index  $n$ . It can be seen from the Fig. 5(a) that when. When  $U = 15 \text{ m/s}$ ,  $n = 0$ , the frequency of the first-order mode  $\omega=2.6643$ , when  $U = 0 \text{ m/s}$ ,  $n = 3.4$ , the frequency of the first-order mode  $\omega=4.115$ , that is, the point with the largest frequency appears in the place where the flow velocity is low and the volume fraction index is small, while the point with the smallest frequency appears in the place where the flow velocity is high and the volume fraction is small.

Figure 6 depicts the change of the critical velocity of the system with the volume fraction index  $n$ . It can be seen from Fig. 6 that when the volume fraction  $n < 10$ , the volume fraction index  $n$  has a great influence on the critical velocity. When  $n > 10$ , the volume fraction index  $n$  is smaller for the critical flow velocity and gradually tends to a fixed value.

It can also be concluded from Fig. 6 that the critical flow rate of the system increases from  $U = 29.3 \text{ m/s}$  when  $n = 0$  to  $U = 56.9 \text{ m/s}$  when  $n = 50$ , and the critical flow

rate increases by 51.5%. In practical engineering applications, the critical flow rate of the system can be improved by adjusting the volume fraction index  $n$ .



**Fig. 6.** Variation of critical velocity with functional gradient fraction exponent  $n$

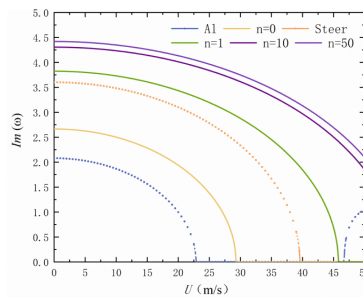


**Fig. 7.** First frequency comparison between functionally Graded materials and conventional materials

Figure 7 is a comparison of the mechanical properties of functionally graded materials and materials commonly used in engineering. From Fig. 7, we can see that functionally graded materials can improve their mechanical properties compared to conventional engineering materials. Compared with aluminum, the mass per unit length of the functionally graded material increases, and its critical flow rate also increases. Compared with steel, the mass per unit length of functionally graded materials is reduced, but the critical flow rate is increased. Therefore, functionally graded materials can improve the stability of the system, which has important guiding significance for the selection of materials in engineering.

Figure 8 shows the modal frequencies with time when the system has an axial velocity of  $v = at$ . In Fig. 8, it can be seen that when the acceleration is large, the critical value of the axial motion of the system is reached faster for the same time with a large acceleration. The stability of the system can be determined by the real and imaginary parts of the intrinsic frequency. When  $\text{Im}(\omega) > 0$  and  $\text{Re}(\omega) = 0$ , the system is in a stable state; while when the acceleration is larger, the time for the intrinsic frequency of the system to converge to 0 is shorter, i.e., the larger the acceleration is, the system is more prone to destabilization with the change of time. By calculating different volume fraction indices

$n$ , it is observed that the larger the volume fraction index, the slower the time for the intrinsic frequency of the system to converge to 0 under the same conditions, i.e., the time for the occurrence of instability is suppressed.

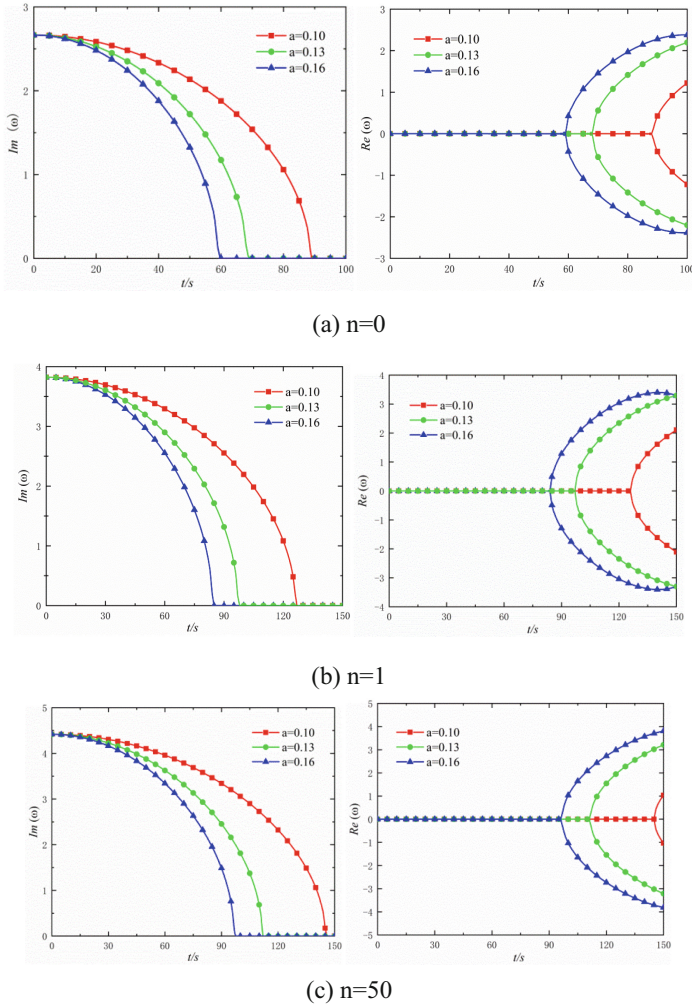


**Fig. 8.** Variation of modal frequency with time under different accelerations

## 5 Conclusion

In this paper, the vibration characteristics of a functional gradient axial kinematic tube are investigated. The critical flow rate and intrinsic frequency of the system are discussed with respect to the volume fraction index  $n$ . Both the critical flow rate and intrinsic

frequency of the system increase with the increase of the volume fraction index  $n$ , and the critical flow rate and intrinsic frequency of the system are more affected when  $n < 10$ . That is, in practical engineering applications, under the condition of knowing the external excitation frequency, the excitation frequency can be avoided by adjusting the volume fraction index  $n$ , so as to reduce the vibration and improve the stability of the system. And through the comparison of mechanical properties of conventional materials and functional gradient materials, it can be found that the functional gradient materials can improve the stability of the system than conventional engineering materials, which is an important guidance for the selection of materials in engineering. When the system exists an acceleration of axial motion, the larger the acceleration, the system will reach the critical value of axial motion tends to be destabilized in the shorter time, and the increase of the volume fraction index  $n$  will inhibit the time for the system to reach the critical velocity, i.e., the stability of the system can be changed by changing the volume fraction index  $n$ .

## References

1. Koizumi, M.: FGM activities in Japan. *Compos. Part B Eng.* **28**(1–2), 1–4 (1997)
2. Birman, V., Byrd, L.W.: Modeling and analysis of functionally graded materials and structures. *Appl. Mech. Rev.* **60**, 195–216 (2007)
3. Tang, Y., Lv, X., Yang, T.: Bi-directional functionally graded beams: asymmetric modes and nonlinear free vibration. *Compos. B Eng.* **156**, 319–331 (2019)
4. Yang, T., Tang, Y., Li, Q., Yang, X.D.: Nonlinear bending, buckling and vibration of bi-directional functionally graded nanobeams. *Compos. Struct.* **204**, 313–319 (2018)
5. Eftekhari, M., Hosseini, M.: On the stability of spinning functionally graded can-tilevered pipes subjected to fluid thermomechanical loading. *Int. J. Struct. Stab. Dyn.* **16**, 1550062 (2016). Selmi, A., Hassis, H.: *Composites Part C: Open Access* **4**, 100117 (2021)
6. Deng, J., Liu, Y., Zhang, Z., Liu, W.: Stability analysis of multi-span viscoelastic functionally graded material pipes conveying fluid using a hybrid method. *Eur. J. Mech. A-Solid* **65**, 257–270 (2017)
7. Tang, T., Yang, T.: Bi-directional functionally graded nanotubes: fluid conveying dynamics. *Int. J. Appl. Mech.* **10**(4), 1850041 (2018)
8. Wang, Z.M., Liu, Y.Z.: Transverse vibration of pipe conveying fluid made of functionally graded materials using a symplectic method. *Nucl. Eng. Des.* **298**, 149–159 (2016)
9. An, C., Su, J.: Dynamic behavior of axially functionally graded pipes conveying fluid. *Math. Probl. Eng.* **2017**, 1–11 (2017)
10. Weiming, L., Hanbin, L., et al.: Influence of moving mass velocity on dynamic response of simply supported beam. *J. Huazhong Univ. Sci. Technol.: Nat. Sci. Ed.* **36**(9), 117–120 (2008)
11. Yinze, W., Xiaobing, Z.: Vibration response analysis of expansion wave launcher with moving mass. *J. Aerodyn.* **24**(8), 1714–1719 (2009)
12. Ning, L., Guolai, Y.: Analysis of vibration characteristics of axially moving cantilever beam with moving mass. *J. Vib. Shock* **31**(3), 106–109 (2012)
13. Wu, J.J., Whittaker, A.R., Cartmell, M.P.: Dynamic responses of structures to moving bodies using combined finite element and analytical methods. *Int. J. Mech. Sci.* **43**, 2555–2579 (2001)
14. Chen, L.-Q., Yang, X.-D.: Nonlinear free transverse vibration of an axially moving beam: comparison of two models. *J. Sound Vib.* **299**(1–2), 348–354 (2007)
15. Ding, H., Chen, L.: On two transverse nonlinear models of axially moving beams. *Sci. China Ser. E: Technol. Sci.* **52**(3), 743–751 (2009). <https://doi.org/10.1007/s11431-009-0060-1>

16. Qi, Y., Liu, N., Yang, G.: Vibration analysis of axially moving simply-supported beam. *J. Ordnance Equipment Eng.* (12), 126–129 (2016)
17. Setoodeh, A.R., Afrahim, S.: Nonlinear dynamic analysis of FG micro-pipes conveying fluid based on strain gradient theory. *Compos. Struct.* **116**, 128–135 (2014)
18. Tang, Y., Yang, T.Z.: Post-buckling behavior and nonlinear vibration analysis of a fluid-conveying pipe composed of functionally graded material. *Compos. Struct.* **185**, 393–400 (2018)
19. Ni, Q., Zhang, Z.L., Wang, L.: Application of the differential transformation method to vibration analysis of pipes conveying fluid. *Appl. Math. Comput.* **217**, 7028–7038 (2011)

**Open Access** This chapter is licensed under the terms of the Creative Commons Attribution 4.0 International License (<http://creativecommons.org/licenses/by/4.0/>), which permits use, sharing, adaptation, distribution and reproduction in any medium or format, as long as you give appropriate credit to the original author(s) and the source, provide a link to the Creative Commons license and indicate if changes were made.

The images or other third party material in this chapter are included in the chapter's Creative Commons license, unless indicated otherwise in a credit line to the material. If material is not included in the chapter's Creative Commons license and your intended use is not permitted by statutory regulation or exceeds the permitted use, you will need to obtain permission directly from the copyright holder.

